PROCEEDINGS OF SCIENCE

Sterile neutrino search with the KATRIN experiment

Leonard Köllenberger[a,*] **for the KATRIN collaboration**

[a] *Institute for Astroparticle Physics (IAP), Karlsruhe Institute of Technology (KIT), Hermann-von-Helmholtz-Platz 1, 76344 Eggenstein-Leopoldshafen, Germany*

E-mail: leonard.koellenberger@kit.edu

The KATRIN experiment is the most precise setup for direct neutrino mass measurements. It is designed and optimised to measure the signature of the neutrino mass in the β-decay spectrum of tritium with a sensitivity of $0.2\,\mathrm{eV/c^2}$ (90 % C.L.) [7].
In addition to the neutrino mass search, the measured β-spectrum can be analysed for an imprint of sterile neutrinos in the eV-range. The first and second KATRIN science runs were taken in 2019. Between these two campaigns, the source activity was substantially increased, leading to improved constraints. No sterile-neutrino signal was observed in the mass range up to 40 eV, and the exclusion contours improved, constraining the active-to-sterile mixing to $|U_{e4}|^2 < 6 \times 10^{-3}$ (95 % C.L.) [2].
With analysis deeper into the spectrum, it is also possible to search for keV-scale sterile neutrinos. During the commissioning phase in 2018, a low source density allowed the opportunity to search for sterile neutrino masses up to 1.6 keV. From this data, mixing amplitudes of $|U_{e4}|^2 < 5 \times 10^{-4}$ (95 % C.L.) are excluded. No sterile neutrino signature was found in the keV-range [3].

8th Symposium on Prospects in the Physics of Discrete Symmetries (DISCRETE 2022)
7-11 November, 2022
Baden-Baden, Germany

*Speaker

PoS(DISCRETE2022)078

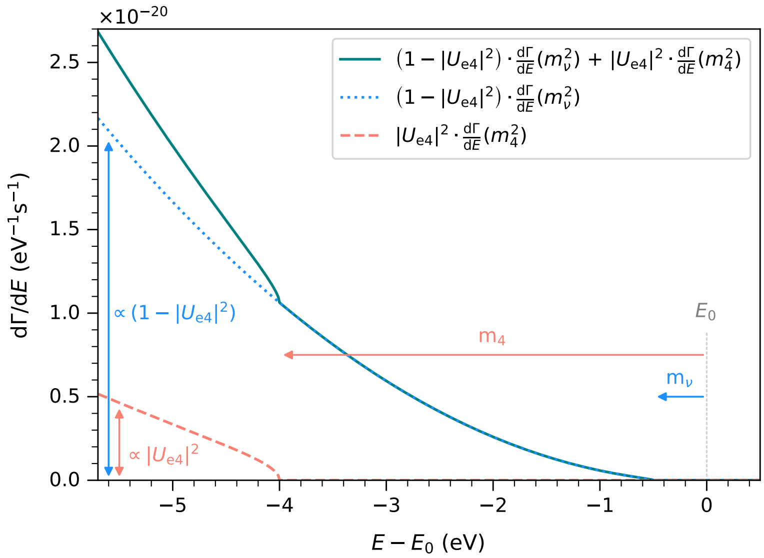

Figure 1: Differential spectrum of the β-decay, including active neutrinos (dotted blue) and sterile neutrinos (dashed orange). The spectra of each branch are shifted by the mass relative to the effective endpoint E_0 (grey). The sum of these spectra gives the combined spectrum (solid teal).

1. The KATRIN experiment

The KATRIN experiment is designed to determine the neutrino mass from kinematic measurements of the β-decay spectrum of molecular tritium. A description of the differential β-decay using Fermi's golden rule leads to the following:

$$\frac{d\Gamma}{dE} = \frac{G_F \cos^2(\Theta_C)}{2\pi^3} \cdot |M_{\text{nucl.}}|^2 \cdot F(Z', E) \cdot p(E + m_e) \cdot \sqrt{(E + m_e)^2 - m_e} \\ \cdot \sum_i |U_{ei}|^2 \cdot (E_0 - E) \cdot \sqrt{(E_0 - E)^2 - m_i^2} \cdot \Theta(E_0 - E - m_i), \tag{1}$$

where E_0 is the endpoint of the tritium spectrum and m_e is the electron mass. $M_{\text{nucl.}}$ corresponds to the matrix element for nuclear transitions. Connected to the leptonic matrix element is the Fermi function $F(Z', E)$. From eq. (5), one can see that the spectral shape is influenced by the squared neutrino mass eigenstates m_i^2. As the mass splitting cannot be resolved by the KATRIN experiment, the observable is the effective squared electron neutrino mass,

$$m_\nu^2 = \sum_{i=1}^{3} |U_{ei}|^2 m_i^2. \tag{2}$$

The formulation of the differential spectrum can also be adapted to account for sterile neutrinos. The $3\nu + 1$ framework is a minimal and well-motivated extension of the standard model. In this

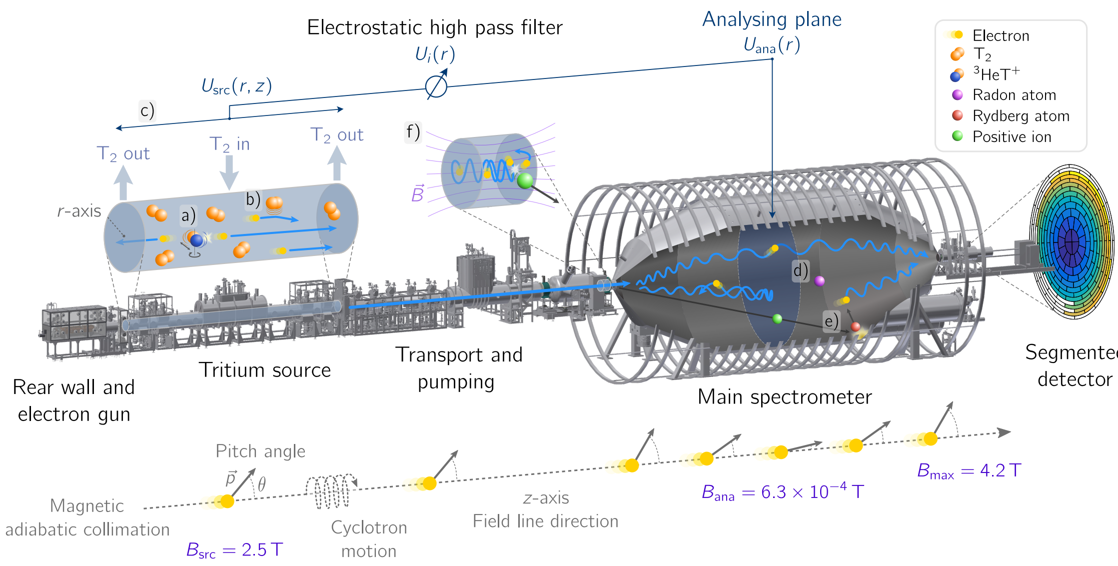

Figure 2: Schematic overview of the working principle of the KATRIN experiment. β-decay electrons generated in the source are magnetically guided into the main spectrometer. Using the MAC-E filter principle, electrons are filtered by their energy. Electrons with sufficient energy can overcome the retarding potential in the main spectrometer and are measured by the detector [1].

case, the sum over the mass eigenstates is extended to also include the heavy, sterile eigenstates,

$$\text{active, light:} \quad \sum_{i,\text{active}} |U_{ei}|^2 =: \cos^2(\theta) \tag{3}$$

$$\text{sterile, heavy:} \quad \sum_{i,\text{sterile}} |U_{ei}|^2 = 1 - \sum_{i,\text{active}} |U_{ei}|^2 =: \sin^2(\theta). \tag{4}$$

This assumes that unitarity is conserved, and the sum of active and sterile branches adds to $\sin^2(\theta) + \cos^2(\theta) = 1$. Summing the spectrum of the active branch and the spectrum of the sterile branch results in the following: (eq. (1))

$$\begin{aligned} \frac{d\Gamma}{dE} &= \cos^2(\theta) \cdot \frac{d\Gamma}{dE}\left(m^2_{\nu_{\text{active}}}\right) + \sin^2(\theta) \cdot \frac{d\Gamma}{dE}\left(m^2_{\nu_{\text{sterile}}}\right) \\ &= (1 - |U_{e4}|^2) \cdot \frac{d\Gamma}{dE}\left(m^2_{\nu}\right) + |U_{e4}|^2 \cdot \frac{d\Gamma}{dE}\left(m^2_4\right). \end{aligned} \tag{5}$$

An illustration of the individual differential spectra and the combined spectrum is shown in fig. 1. The addition of sterile neutrinos is manifested in a characteristic kink-like signature within the measured spectrum. The kink position corresponds to the sterile mass m_4, and the sterile-to-active mixing is proportional to the amplitude of the additional spectrum.

To measure the spectral shape, the main spectrometer of the KATRIN experiment functions Magnetic Adiabatic Collimation combined with an Electrostatic (MAC-E) filter. The MAC-E filter concept was originally introduced by Picard et al. in 1992 [11] following the work of Beamson et al.[4] and Kruit et al. [9]. The working principle of a MAC-E filter is based on a special combination of magnetic and electric fields, functioning as a highpass filter for charged particles. A schematic overview of the KATRIN experiment and its working principle is shown in fig. 2. Decay electrons

PoS(DISCRETE2022)078

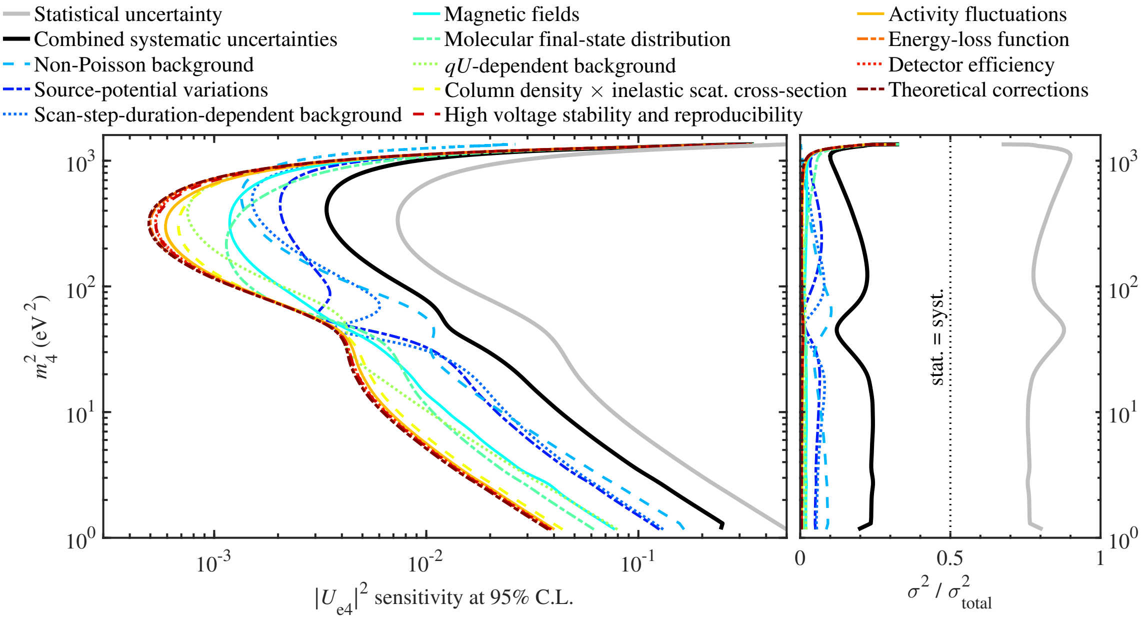

Figure 3: Systematic breakdown of KNM2. The systematic impact is estimated from a raster scan. In the left panel, the individual contribution of systematic effects is estimated by $\sigma_{sys.} = \sqrt{\sigma^2_{stat.\&sys.} - \sigma^2_{stat.}}$. In addition to this, the relative contribution is illustrated in the right panel. The exclusion is dominated by statistical uncertainties [2].

are magnetically guided from the source into the main spectrometer. By decreasing the magnetic field, transversal momentum is transformed into the longitudinal direction. An opposing retarding potential, decelerates the electrons. Electrons with sufficient energy can overcome the potential and are measured with the focal plane detector at the end of the experimental setup.

Combining the response function $R(E, qU)$ to describe the transport through the KATRIN beamline and the predicted differential spectrum of molecular tritium, the integrated rate of β-electrons $\dot{N}_{sig}(qU)$ is calculated,

$$\dot{N}_{sig}(qU) = \mathrm{Sig} \cdot N_T \cdot \frac{\Omega}{4\pi} \int_{qU}^{E_0} \frac{d\Gamma}{dE} \cdot R(E, qU)\, dE\,. \tag{6}$$

2. eV-scale sterile neutrino analysis

The search for eV-scale sterile neutrinos is motivated by long-standing anomalies in the short baseline and oscillation experiments. During the first KATRIN measurement campaign, 274 scans with a total of 2.03×10^6 electrons were recorded by the 117 active pixels. During the second KATRIN measurement campaign, 361 scans with a total of 4.17×10^6 electrons were recorded by the 117 active pixels. In the following, the first and second neutrino mass campaigns will be referred to as KNM1 and KNM2. The spectra of the individual scans within each campaign are stacked into one spectrum.

PoS(DISCRETE2022)078

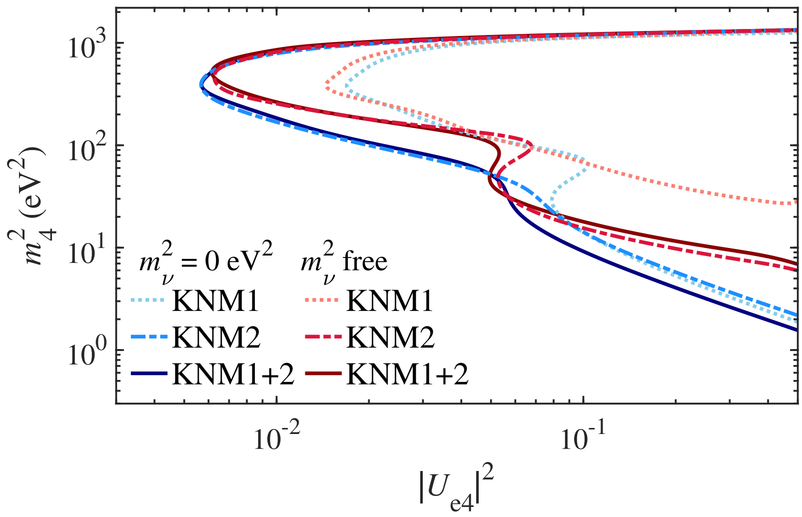

Figure 4: Summary of the 95 % C.L. exclusion contours from KNM1, KNM2, and the KNM1+2 combined analysis (blue). The impact on the exclusion contour when adding a free active neutrino mass is shown (red) [2].

For the inference of the sterile-neutrino parameters a grid scan over the parameter space m_4^2 and $|U_{e4}|^2$ is applied. 95 % C.L. exclusion contours are calculated following Wilk's theorem [12], where $\Delta\chi^2 = \chi^2 - \chi^2_{\text{min}} = 5.99$.

Systematic uncertainties are propagated into the analysis via the covariance matrix approach. The impact of each individual systematic effect taken into account in the KNM2 analysis is illustrated in fig. 3. The impact is estimated by a raster scan on a simulated data set. This shows that the analysis is statistics dominated over the entire mass range.

The 95 % C.L. exclusion contours of KNM1, KNM2, and the combined KNM1+2 analysis on the $(m_4^2, |U_{e4}|^2)$ parameter space are shown in fig. 4. The figure includes the results when analysing the data with an active neutrino mass fixed to $m_\nu^2 = 0\,\text{eV}^2$ (blue) and a free active mass (red). For the KNM1+2 analysis we find a best fit at $(m_4^2 = 59.9\,\text{eV}^2, |U_{e4}|^2 = 0.011)$ with 28 % significance which is compatible with the null hypothesis. Structures in the exclusion contours are explained by the location of the best fit. The analysis is sensitive to an active-to-sterile mixing of $|U_{e4}|^2 \gtrsim 6 \times 10^{-3}$. [2]

To place the KATRIN results into the context of other experiments, the contours are transformed into the parameter space accessible to oscillation experiments: $\sin^2(2\theta_{ee}) = 4|U_{e4}|^2(1 - |U_{e4}|^2)$ and $\Delta m_4^2 \approx m_4^2 - m_\nu^2$. In the scenario where $m_\nu^2 = 0\,\text{eV}^2$, the mass splitting is approximated by $\Delta m_4^2 \approx m_4$. These results are displayed in fig. 5. The KNM1+2 exclusion contour (dark blue) improves on the previous limits from the Mainz [8] and Troitsk [5] experiments for $m_4^2 \lesssim 300\,\text{eV}^2$. This result disfavours parts of the Neutrino-4 signal for $\sin^2(2\theta_{ee}) \gtrsim 0.4$ [13]. Furthermore, large solutions of the reactor antineutrino anomaly (RAA) [10] and galium anomalies (BEST+GA) [14] are excluded. In addition, the KATRIN experiment improves on short-baseline experiment exclusion bounds for $\Delta m_4^2 \gtrsim 10\,\text{eV}^2$. With more measurement time, the sensitivity is expected to improve by a factor of 50. [2]

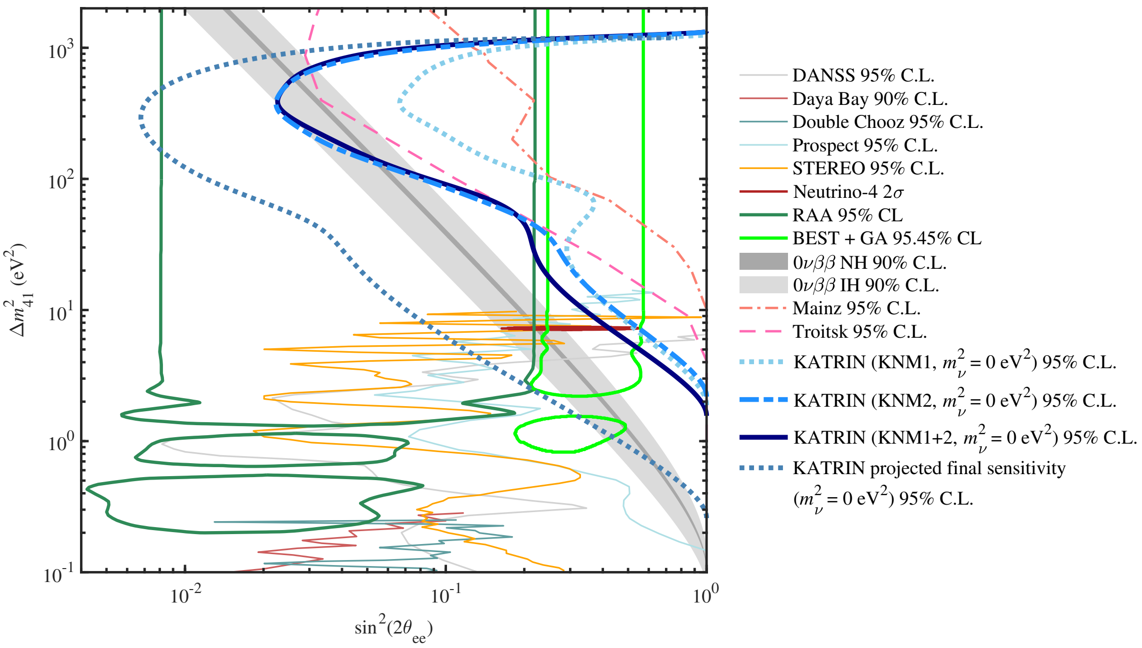

Figure 5: 95 % C.L. exclusion contour of the sterile neutrino analysis of the first two campaigns (blue) and projected sensitivity for 1000 days of data taking. The KATRIN contours are compared to results from oscillation experiments, such as the galium anomaly (GA) and reactor antineutrino anomaly (RAA), neutrinoless double beta decay, and previous β decay experiments [2].

3. keV-scale sterile neutrino analysis

Sterile neutrinos in the keV-range are viable candidates for warm dark matter [6]. During the first tritium commissioning campaign in 2018, a total of 1.2×10^9 electrons were recorded, down to 1.6 keV below the endpoint. When analysing deeper into the spectrum, additional systematic effects have to be accounted for. In addition to the standard systematic effects used in the eV range analysis, corrections and uncertainties for decays within magnetic traps, backscattering of electrons from the rear wall, and detection efficiency are applied in the analysis of the data set. The results of the keV-range analysis are shown in fig. 6. Here, contours are also constructed from a grid scan. The excluded parameter space is shown relative to the null hypothesis (orange) and relative to the best fit (blue). The best fit was found at $m_4 = 71.2$ eV and $\sin^2\theta = 0.017$ with a significance of 92 %. The analysis improves on previous laboratory limits in a range between 0.1 keV $< m_4 <$ 1.0 keV. From this data mixing amplitudes $|U_{e4}|^2 < 5 \times 10^{-4}$ (95 % C.L.) can be excluded. [3]

4. Conclusion

Analysing the KNM1 and KNM2 data sets yields an improved exclusion limit in the sterile neutrino mass range up to 40 eV. The active-to-sterile scaling can further be constrained down to $|U_{e4}|^2 < 6 \times 10^{-3}$. The result excludes large solutions of the RAA and GA, and parts of the Neutrino-4 solution at 95 % C.L. [2].

In addition, the first search for keV-scale sterile neutrinos was performed with the KATRIN experiment. The analysis improves on results of previous laboratory experiments [3]. The result

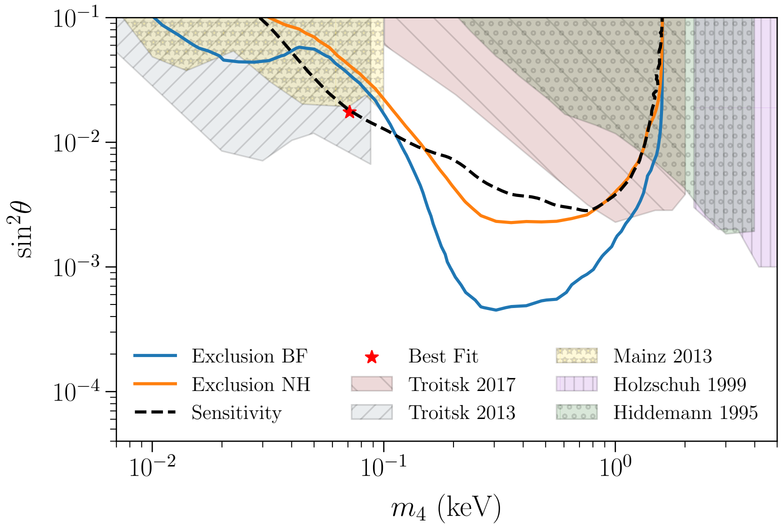

Figure 6: 95 % C.L. exclusion limit based on the first tritium commissioning campaign. The contours are shown relative to the best fit (blue) and the null hypothesis (orange). [3].

establishes a first milestone in the search for keV sterile neutrinos with KATRIN. This is especially important groundwork for the future TRISTAN detector upgrade, which is currently in development. The novel detector system will enable the search for sterile neutrinos with KATRIN in a wider energy range.

Acknowledgements

We acknowledge the support of Helmholtz Association (HGF); Ministry for Education and Research BMBF (05A17PM3, 05A17PX3, 05A17VK2, 05A17PDA, 05A17WO3, 05A20VK3, 05A20PMA and 05A20PX3); Helmholtz Alliance for Astroparticle Physics (HAP); the doctoral school KSETA at KIT; Helmholtz Young Investigator Group (VH-NG-1055); Max Planck Research Group (MaxPlanck@TUM); Deutsche Forschungsgemeinschaft DFG (Research Training Group grant nos. GRK 1694 and GRK 2149); Graduate School grant no. GSC 1085-KSETA, SFB-1258, and Excellence Cluster ORIGINS in Germany; Ministry of Education, Youth and Sport (CANAM-LM2015056, LTT19005) in the Czech Republic; the Department of Energy through grants DE-FG02-97ER41020, DE-FG02-94ER40818, DE-SC0004036, DE-FG02-97ER41033, DE-FG02-97ER41041, DE-SC0011091 and DE-SC0019304; and the Federal Prime Agreement DE-AC02-05CH11231 in the USA. This project has received funding from the European Research Council (ERC) under the European Union Horizon 2020 research and innovation programme (grant agreement no. 852845). We thank the computing cluster support at the Institute for Astroparticle Physics at Karlsruhe Institute of Technology, Max Planck Computing and Data Facility (MPCDF), and National Energy Research Scientific Computing Center (NERSC) at Lawrence Berkeley National Laboratory.

References

[1] M. Aker et al. (2022) *Direct neutrino-mass measurement with sub-electronvolt sensitivity*, *Nature Physics* **18** (2) pp. 160–166

[2] M. Aker et al. (2022) *Improved eV-scale sterile-neutrino constraints from the second KATRIN measurement campaign*, *Physical Review D* **105** (7) 2004

[3] M. Aker et al. (2022) *Search for keV-scale Sterile Neutrinos with first KATRIN Data*, arXiv:2207.06337

[4] G. Beamson and H. Q. Porter and D. W. Turner (Jan. 1980) *The collimating and magnifying properties of a superconducting field photoelectron spectrometer*, *Nuclear Instruments and Methods in Physics Research Section B* **13** (1) pp. 64–66

[5] A. I. Belesev et al. (2013) *An upper limit on additional neutrino mass eigenstate in 2 to 100 eV region from 'Troitsk nu-mass' data*, *JETP Letters* **97** pp. 67-–69

[6] M. Drewes et al. (2017) *A White Paper on keV sterile neutrino Dark Matter*, *Journal of Cosmology and Astroparticle Physics* **1701** 025

[7] The KATRIN Collaboration (2005) *KATRIN design report 2004*, *Wissenschaftliche Berichte. FZKA* **7090**

[8] C. Kraus, A. Singer, K. Valerius, and C. Weinheimer (2013) *Limit on sterile neutrino contribution from the Mainz Neutrino Mass Experiment*, *The European Physical Journal C* **73** 2323

[9] P. Kruit and F. H. Read (1983) *Magnetic field paralleliser for 2π electron-spectrometer and electron-image magnifier*, *Journal of Physics E* **16** (4) pp. 313–324

[10] G. Mention et al. (2011) *The reactor antineutrino anomaly*, *Physical Review D* **83** (7) 073006

[11] A. Picard et al. (1992) *A solenoid retarding spectrometer with high resolution and transmission for keV electrons*, *Nuclear Instruments and Methods in Physics Research Section B* **63** (3) pp. 345–358

[12] S. S. Wilks (1938) *The Large-Sample Distribution of the Likelihood Ratio for Testing Composite Hypotheses*, *The Annals of Mathematical Statistics* **9** (1) pp. 60–62

[13] A. P. Serebrov et al. (2019) *First observation of the oscillation effect in the neutrino-4 experiment on the search for the sterile neutrino* *Pis'ma Zh. Eksp. Teor. Fiz.* **109** pp- 209–218

[14] V. V. Barinov et al. (2022) *Results from the Baksan Experiment on Sterile Transitions (BEST)*, *Phys. Rev. Lett.* **128** (23) 232501